COBEM 2023 27TH INTERNATIONAL CONGRESS OF MECHANICAL ENGINEERING

ABCM Brazilian Society of Mechanical Sciences and Engineering
27th ABCM International Congress of Mechanical Engineering
December 04-08, 2023, Florianópolis-SC, Brazil

COB-2023-1358
ISOGEOMETRIC ANALYSIS IN SOLID MECHANICS: EXPLORING PRECISION AND VERSATILITY

Beatriz Corchak Veiga
Roberto Dalledone Machado
Graduate Program in Civil Engineering, Federal University of Paraná – UFPR, Curitiba, Brazil
beatrizveiga@ufpr.br
rdm@ufpr.br

Abstract. *This research investigates the application of Isogeometric Analysis (IGA) in solid mechanics, particularly in plane stress analysis. It aims to evaluate the effectiveness of IGA compared to the Finite Element Method (FEM) and analytical solutions. IGA combines precise geometry modeling with accurate numerical analysis, enabling the modeling of complex surfaces and integration with CAD and CAE systems. It offers improved accuracy and efficiency in structural applications where traditional FEM may have limitations. The study explores different enrichment techniques, including h-refinement, p-refinement, and k-refinement, to enhance numerical solutions, accuracy, and efficiency. By implementing IGA with NURBS basis functions and conducting numerical simulations, the research analyzes structural behavior under plane stress conditions. The results highlight the superior accuracy achieved by k-refinement compared to hp-refinement, emphasizing the significance of control point distribution. Moreover, IGA demonstrates its capability to accurately reproduce stress distributions in problems, such as plate with central hole, similar to analytical solutions. Overall, this research advances the understanding and application of Isogeometric Analysis in solid mechanics, showcasing its potential as a robust tool for precise and efficient numerical modeling in engineering practice.*

Keywords: *Isogeometric Analysis, solid mechanis, plane stress, refinement*

1. INTRODUCTION

The development of modern engineering projects involves fundamental stages, including graphical representation, numerical model creation, analysis, problem resolution, and post-processing. Discretization based on approximate Computer-Aided Design (CAD) geometry may introduce inaccuracies due to element shape during discretization, as observed in the Finite Element Method (FEM), consequently leading to geometric errors in the numerical solution.

To address this issue, the concept of Isogeometric Analysis (IGA) was introduced, initially proposed by Hughes;Cottrell; Bazilevs (2005). This innovative approach aims to integrate the CAD and CAE (Computer-Aided Engineering) environments through the utilization of Non-Uniform Rational B-Splines (NURBS), which are equations characterized by the CAD environment.NURBS are employed to describe both the geometry and the approximation of the analyzed field, sharing common characteristics with the FEM.

Numerical efficiency has been demonstrated through testing on various structural mechanics problems. The pioneering application of IGA to structural vibration problems, including Euler-Bernoulli beams, membranes, and plates, is detailed in Cottrell et al.'s study (2006), showcasing superior performance compared to classical FEM polynomials like Hermite polynomials.

Several mesh refinement schemes have been studied, including h-refinement, p-refinement, and a newly proposed krefinement. Important properties of IGA in refinement were explored by Cottrell; Hughes; Reali (2007), with a foundational book on this topic developed later Cottrell; Bazilevs; Hughes, 2009).

In this study, IGA is applied to investigate problems in the plane stress state within the linear-elastic regime. Initially, the analysis focuses on the displacement of a clamped beam under distributed loading. The objective is to present a numerical example considering unit weights and analyze its behavior with respect to various refinements (h, p, and k). Subsequently, the study focuses on the analysis of a plate with a circular hole under constant in-plane tension, evaluating the stress concentration around the hole using k-refinement.

2. A BRIEF INTRODUCTION TO NURBS

Isogeometric Analysis is based on the utilization of NURBS basis functions, which describe the geometry and approximation of the field under analysis. To better understand these functions, it is necessary to begin studying B-Spline functions, which will be addressed subsequently.

2.1 B-Splines

For the understanding of B-Splines, we must first address the knot vector. In one dimension, the knot vector $\Xi = \{\xi_1, \xi_2, \ldots, \xi_{n+p+1}\}$ consists of non-decreasing coordinates in the parametric space. Each $\xi_i \in \mathbb{R}$ represents the i^{th} knot.Where i is the knot index ranging from 1 to $n + p + 1$. The polynomial order is denoted by p, and n represents the number of basis functions used for the B-Spline curve representation.

Knots divide the parameter space into elements, and their boundaries in physical space are images of the knot lines under the B-Spline mapping. Knot vectors can be either uniform or non-uniform. A uniform knot vector has equally spaced knots in the parameter space, like $\Xi = \{0, 1, 2, 3, 4\}$. If the knots are not equally spaced, the knot vector is considered non-uniform, for example, $\Xi = \{0, 0, 0, 1, 1, 2, 3, 4, 4, 4\}$. Knots can also be repeated, for example, $\Xi = \{0, 0, 0, 0.5, 0.5, 1, 1, 1\}$, where increasing the multiplicity affects continuity. Non-uniform knot vectors are preferred for better behavior compared to uniform ones (Cottrell; Bazilevs; Hughes, 2009).

The multiplicity of a knot refers to how many times it appears in the knot vector and is directly related to the continuity of the B-Spline curve, surface, or volume. Continuity is denoted as C_{p-m}, determined by the polynomial order p and the number of times the knot appears m.

Knot vectors can also be classified as open or non-open. An open knot vector has the first and last coordinates appearing $p + 1$ times, corresponding to a multiplicity of $p + 1$. This pattern is commonly used in CAD literature and allows defining nodal degrees of freedom at the element ends.

Given a knot vector, the B-Spline basis functions are constructed recursively using the Cox-de Boor recursive formula (Cox, 1971; de Boor, 1972). The construction begins with a polynomial degree of $p = 0$:

$$N_{i,0}(\xi) = \begin{cases} 1 & \text{if } \xi_i < \xi \leq \xi_{i+1} \\ 0 & \text{otherwise} \end{cases} \tag{1}$$

The subsequent iterations for $p = 1, 2, 3, \ldots$ are given by:

$$N_{i,p}(\xi) = \frac{\xi - \xi_i}{\xi_{i+p} - \xi_i} N_{i,p-1}(\xi) + \frac{\xi_{i+p+1} - \xi}{\xi_{i+p+1} - \xi_{i+1}} N_{i+1,p-1}(\xi) \tag{2}$$

The Figure 1 illustrates the configuration of B-Spline functions through a knot vector and the continuity conditions for each knot.

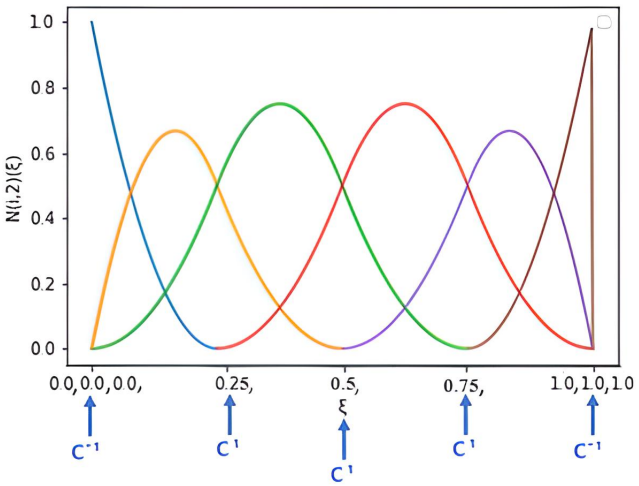

Figure 1. Quadratic B-Splines for the knot vector $\Xi = \{0, 0, 0, 0.25, 0.5, 0.75, 1, 1, 1\}$ and their continuities.

By employing a linear combination of the basis functions, one can obtain B-Spline curves, which are defined as follows:

$$C(\xi) = \sum_{i=1}^{n} N_{i,p}(\xi) \mathbf{B}_i \tag{3}$$

Where $\mathbf{B}_i \in \mathbb{R}^d$, $i = 1, 2, \ldots, n$, are the coefficients known as control points. The linear interpolation of these control points generates the so-called control polygon. A B-Spline curve is illustrated in Figure 2.

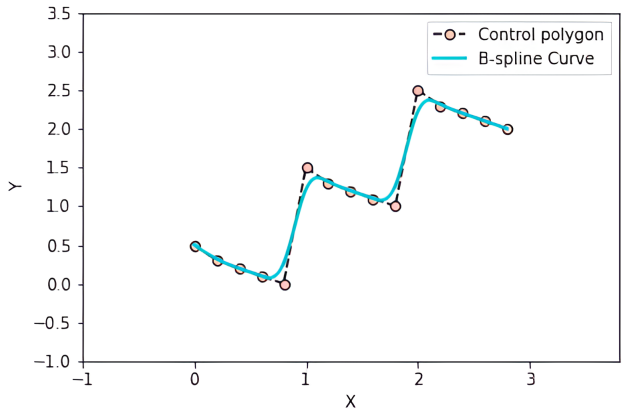

Figure 2. Quadratic B-Spline curve and its corresponding control polygon.

Figure 3 illustrates a quadratic B-spline surface.Therefore, given a control mesh $\{\mathbf{B}_{i,j}\}, i = 1, 2, \ldots, n; j = 1, 2, \ldots, m$, polynomial orders p and q, knot vectors $\Xi = \{\xi_1, \xi_2, \ldots, \xi_{n+p+1}\}$ and $\mathcal{H} = \{\eta_1, \eta_2, \ldots, \eta_{m+q+1}\}$, and B-Spline basis functions in each direction $N_{i,p}(\xi)$ and $M_{j,q}(\eta)$, the B-spline surface is defined as follows:

$$S(\xi, \eta) = \sum_{j=1}^{m} \sum_{i=1}^{n} N_{i,p}(\xi) M_{j,q}(\eta) \mathbf{B}_{i,j} \tag{4}$$

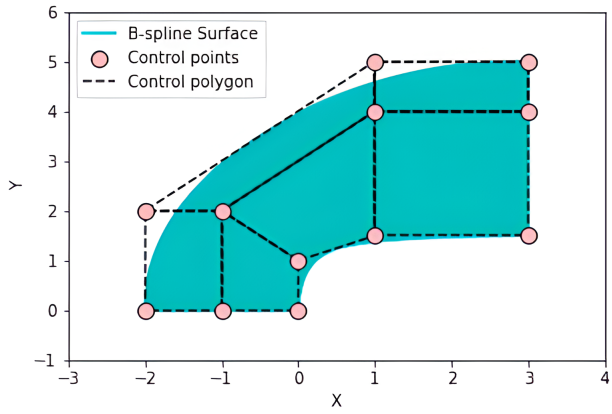

Figure 3. Quadratic B-Spline surface and its corresponding control polygon.

2.2 NURBS Basis Functions

NURBS functions represent an extension of B-splines that introduce a weight parameter w_i, providing greater flexibility in geometric constructions. To obtain a NURBS entity in $\mathbb{R}^d$, a projective transformation is performed on a B-spline entity in $\mathbb{R}^{d+1}$ (Cottrell; Bazilevs; Hughes ,2009). The rational basis functions and NURBS curves are expressed by Eq. (5) and Eq. (6), respectively:

$$R_{i,p}(\xi) = \frac{N_{i,p}(\xi) w_i}{W(\xi)} \tag{5}$$

$$C(\xi) = \sum_{i=1}^{n} R_{i,p}(\xi) B_i \tag{6}$$

Where $W(\xi)$ is the weighted sum of B-Spline basis functions at all control points. Rational surfaces can be defined in a similar manner in terms of rational functions.

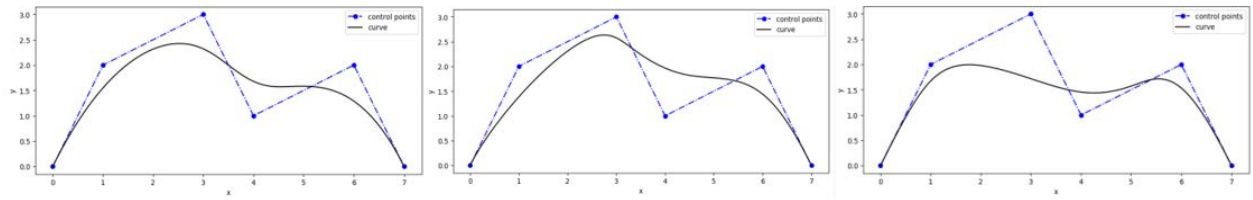

Figure 4. Cubic NURBS curves with weight variation and knot vector $\Xi = \{0, 0, 0, 0, 1/3, 2/3, 1, 1, 1, 1\}$.

$$R_{i,p}(\xi,\eta)_j^q = \frac{N_{i,p}(\xi)M_{j,q}(\eta)w_{i,j}}{W(\xi,\eta)} \tag{7}$$

It is important to emphasize that if the weights are equal, NURBS curves reduce to B-splines. Figure 4 illustrates the impact of weight values on the geometry of the NURBS curve, highlighting their influence on the curve's shape and behavior.

3. MAIN CONCEPTS OF ISOGEOMETRIC ANALYSIS

3.1 Mesh Concepts and Parametric Space

According to Cottrell; Bazilevs; Hughes (2009), in IGA, there are two mesh concepts: the control mesh and the physical mesh. The control mesh consists of multilinear elements that interpolate the control points defining the mesh. In 2D, these elements are quadrilateral bilinear elements. The mesh does not conform to the actual geometry but serves as a scaffold to control it, potentially causing significant distortion. Degrees of freedom are associated with the control points.

The physical mesh is obtained by decomposing the actual geometry in physical space using two elementary notions: patch and knot span. The patch represents a macro element or subdomain, simplifying geometries for numerical analyses on a single patch. In the parametric space, the patch is formed by applying NURBS functions, represented by a 2D rectangle in the coordinate system Ξ and η. Thus, the parametric space is a compact index space, including only elements contributing to the numerical analysis.

Each patch can be subdivided into knot spans, small elements where intervals between knots are represented by points in 1D and lines in 2D. Consequently, the physical mesh in physical space is formed by the union of successive knot spans, suitably mapped. The accompanying figure provides a visual representation of these concepts.

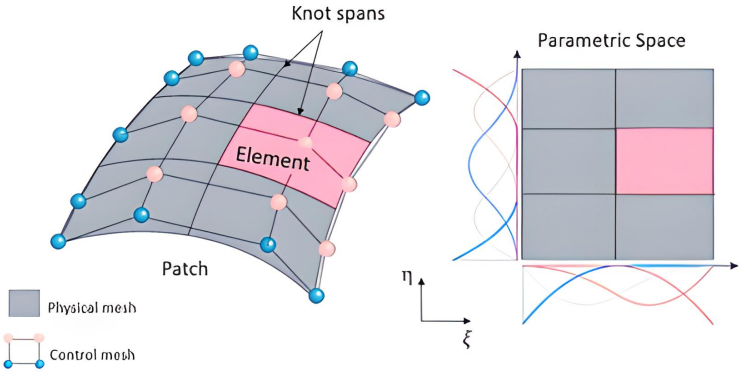

Figure 5. Patch with physical and control mesh, parametric space representation (Adapted from Klinkel, 2018).

3.2 Index Space

The index space is formed by intersecting knots from the knot vectors Ξ and $\mathcal{H}$, creating a rectangular grid with elements from the knot spans, including those with zero and non-zero areas. It defines connectivity matrices INC and IEN, crucial for global and local numbering of functions. Global numbering positions functions relative to all others, while local numbering identifies positions relative to immediate neighbors.

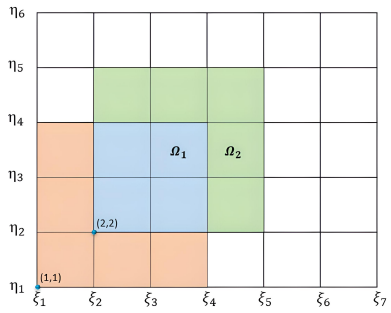

Figure 6. Index space of a patch. (Adapted from Cottrell; Bazilevs; Hughes, 2009)

3.3 Parent Space

The parent space is necessary for numerical integration. In this study, the integration interval for Gaussian quadrature, referred to as the interval $[-1, 1]$, is determined by the coordinate system $\tilde{\xi}$ and $\tilde{\eta}$.

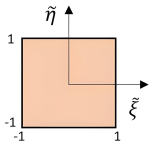

Figure 7. Parent space. (Adapted from Cottrell; Bazilevs; Hughes, 2009)

3.4 Mappings

To perform integrations using Gaussian quadrature, two distinct mappings are required. The first one is the geometric mapping $\mathbf{x} : \hat{\Omega} \rightarrow \Omega$, representing the mapping from the parametric space to the physical space. This mapping is inverted as $\mathbf{x}^{-1} : \Omega \rightarrow \hat{\Omega}$, allowing mapping of an element from the physical space Ω_e to the parametric space $\hat{\Omega}_e$.

The second mapping is the affine mapping $\Phi : \tilde{\Omega} \rightarrow \hat{\Omega}$, responsible for mapping the integration domain to the parametric space. This mapping is also inverted as $\Phi^{-1} : \hat{\Omega} \rightarrow \tilde{\Omega}$, enabling mapping of an element in the parametric space $\hat{\Omega}_e$ to the integration domain $\tilde{\Omega}_e$. Thus, mapping a physical element Ω_e to an element in the integration domain $\tilde{\Omega}_e$ requires the composition of the inverted mappings: $\mathbf{x}^{-1}$ and Φ^{-1}.

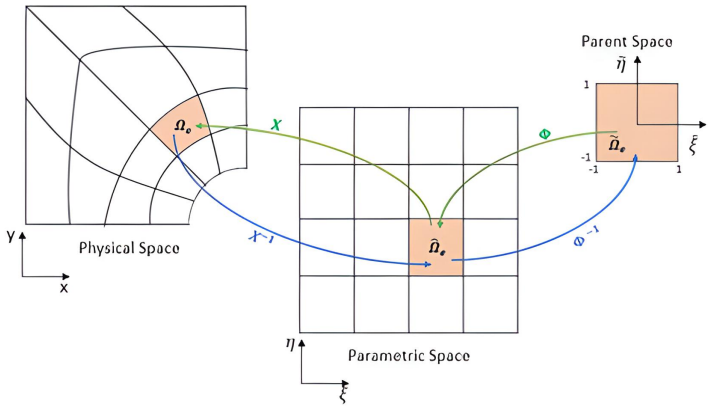

Figure 8. Mappings

4. IGA REFINEMENTS

From the perspective of shape functions, IGA refinement involves adjusting the parameters of the functions. Modifying the input parameters Ξ, n, and p creates a new set of shape functions, corresponding to various types of refinements.

Isogeometric h-refinement enhances accuracy and precision by adjusting parameters n and Ξ. Increasing the number of shape functions (n) intensifies refinement, requiring the addition of knots in the parameter vector Ξ, refining the geometry representation. This results in a more detailed and accurate analysis. The illustration below showcases the representation of h-refinement in NURBS curve.

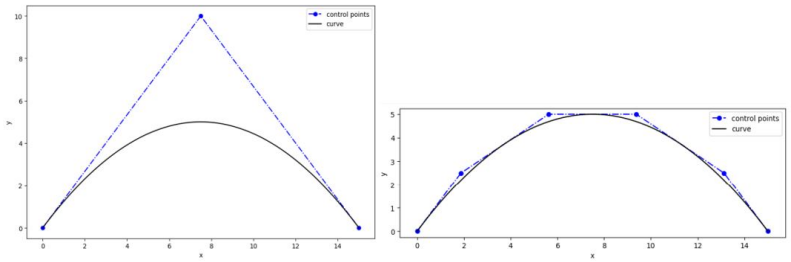

Figure 9. h-refinement of NURBS curve.

Isogeometric p-refinement involves increasing the polynomial order while maintaining continuity and increasing the number of shape functions (n). The knot vector is also affected, with all knots having increased multiplicity. Further details can be found in the works of Cottrell; Hughes; Reali (2007) and Cottrell; Bazilevs; Hughes (2009). Figure 10 illustrates p-refinement, where the NURBS curve's initial degree was $p = 2$, then increased to $p = 4$.

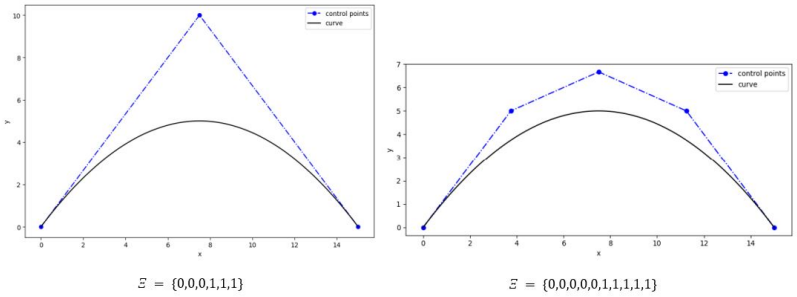

Figure 10. p-refinement of NURBS curve.

The k-refinement increases the polynomial degree while maintaining the multiplicity of interior knots, ensuring high continuity within the element domain. Unlike other refinements, it always starts from the coarsest or initial mesh at each level (Cottrell;Hughes;Reali 2007). Figure 11 illustrates this process in a NURBS curve.

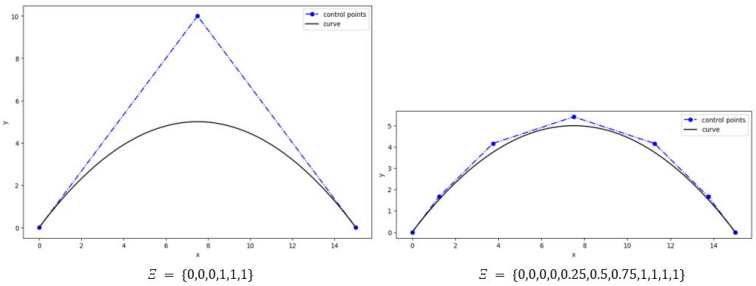

Figure 11. k-refinement of NURBS curve.

5. RESULTS

In this section, we present and discuss the results obtained for problems involving plane stress conditions using Isogeometric Analysis. For this particular type of problem, we utilize the following constitutive matrix:

$$\mathbf{D} = \frac{E}{(1-\nu^2)} \begin{bmatrix} 1 & \nu & 0 \\ \nu & 1 & 0 \\ 0 & 0 & \frac{(1-\nu)}{2} \end{bmatrix} \tag{8}$$

In this equation, E represents the modulus of elasticity, and ν denotes the coefficient of Poisson. To address the system $Ku = f$ utilizing Gaussian quadrature, we utilize the following configurations:

$$K_e = \sum_{i=1}^{n_{PG}^{\xi}} \sum_{j=1}^{n_{PG}^{\eta}} W_i W_j B^T D B \frac{1}{|J|} \tag{9}$$

$$\bar{f}_e = \sum_{i=1}^{n_{PG}^{\xi}} W_i \bar{q}_i^{\xi} \sqrt{\left(\frac{dx}{d\xi}\right)_{\eta}^2 + \left(\frac{dy}{d\xi}\right)_{\eta}^2} \quad \text{or} \quad \bar{f}_e = \sum_{j=1}^{n_{PG}^{\eta}} W_j \bar{q}_j^{\eta} \sqrt{\left(\frac{dx}{d\eta}\right)_{\xi}^2 + \left(\frac{dy}{d\eta}\right)_{\xi}^2} \tag{10}$$

In Eq. (9), K_e represents the elemental stiffness matrix, while Eq. (10) denotes the surface force vector as $\bar{f}_e$. Here, W_i and W_j represent the Gauss weights, q is the applied load, and ξ and η are the coordinates in the parametric space.

5.1 Clamped beam under distributed load

Through a plane stress analysis, it is possible to calculate the resulting displacements in a clamped beam subjected to distributed loading. Figure 12 illustrates the configuration of the beam under study.

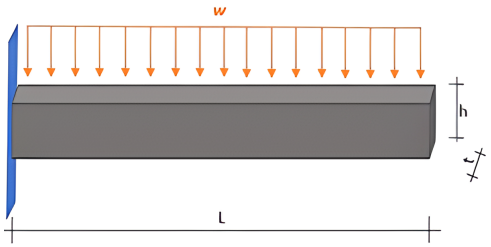

Figure 12. Configuration of the studied beam.

The beam used in this study has a height (h) of 1.1 meters, a length (L) of 4.7 meters, and a thickness (t) of 0.2 meters. It is subjected to a distributed loading of 150 kN/m. Additional material parameters are provided, including a modulus of elasticity (E) of 2×10^7 kN/m² and a Poisson's ratio of 0.25. Figure 13(a) shows the displacement configuration in the y-axis obtained through the FEM using FEMAP software and 2250 bilinear elements. Figure 13(b) presents the y-displacement configuration obtained through k-refinement using 280 cubic isogeometric elements.

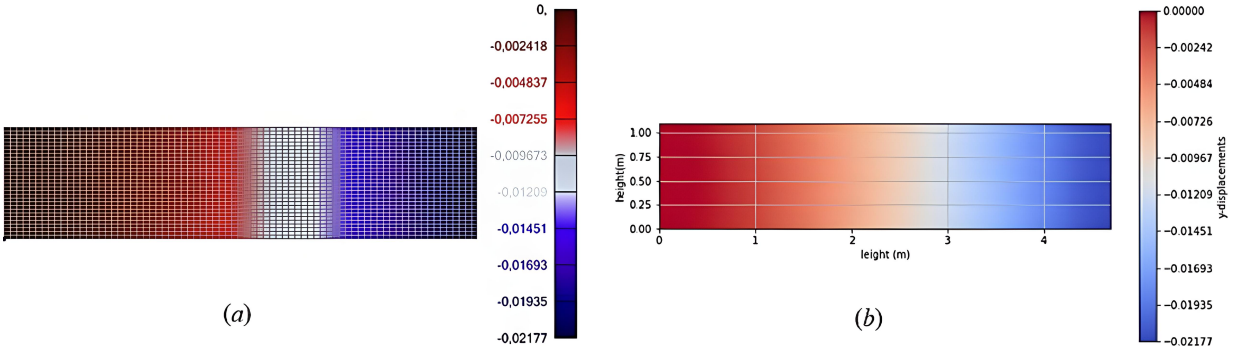

Figure 13. (a) y-displacements FEMAP. (b) y-displacements k-refinement.

To evaluate the results, a convergence analysis of the maximum y-displacement of the beam was performed using hp and k refinement, along with a liner distribution of control points identical to the characteristic mesh of FEM. The following figure allows for a comparison between the finest mesh used in k-refinement: (a) its control point mesh by Isogeometric Analysis and (b) its control point mesh equally divided, analogous to the typical Finite Element mesh. It is important to note that unit weights were used in this study due to the simplicity of its geometry.

Subsequently, the convergence graph of the maximum displacement in each refinement is presented.

Therefore, it can be concluded that, as expected, k-refinement achieved the finer response in FEM earlier than hp-refinement due to its smoothness. Furthermore, it is important to highlight that the distribution of control points significantly affects the results, as the accuracy of k-refinement with a mesh with linear distribution of control points deteriorated when compared to k-refinement with isogeometric mesh.

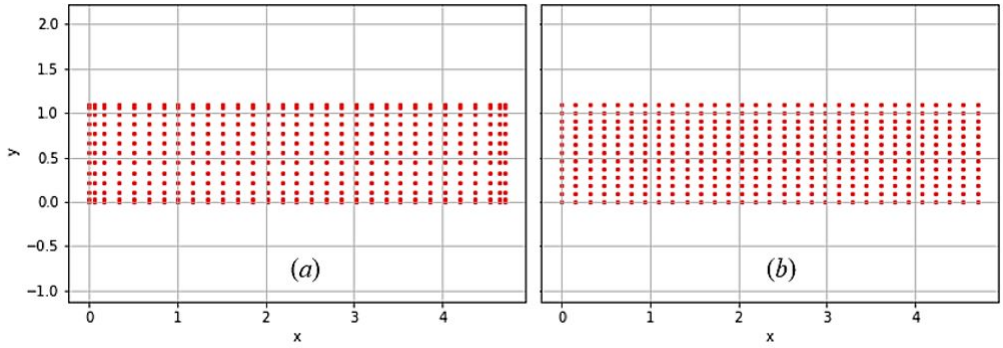

Figure 14. (a) k-refinement isogeometric mesh. (b) k-refinement linear isogeometric mesh.

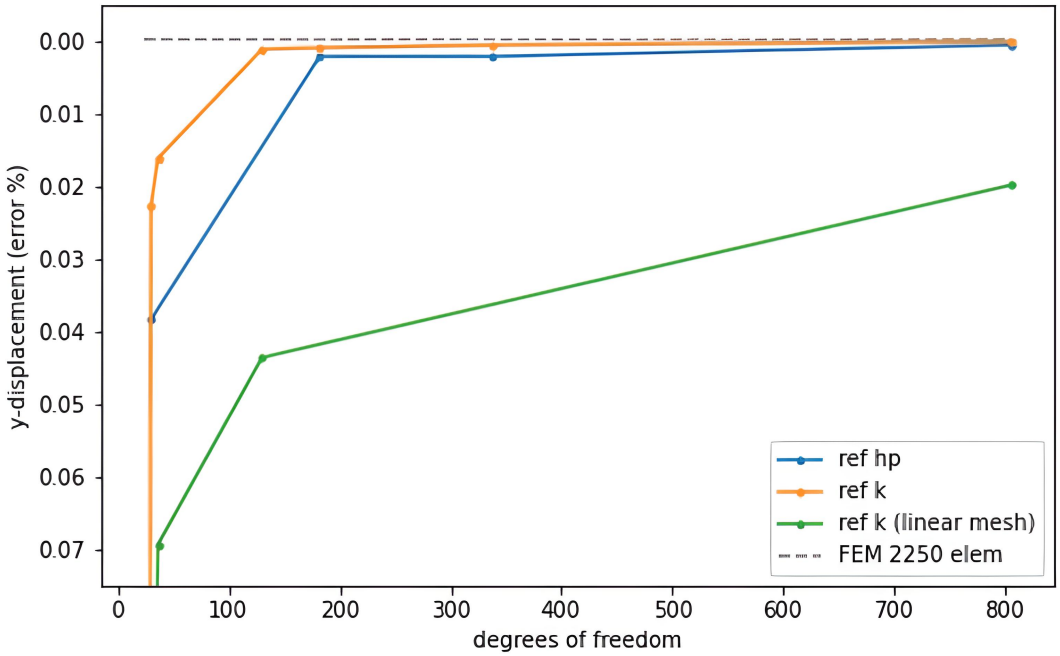

Figure 15. Convergence plot for maximum y-displacement of the beam.

5.2 Infinite plate with a circular hole under constant in-plane tension

To investigate more complex geometries, the analysis was directed towards a plate with a central circular hole subjected to constant in-plane tension (Hughes; Cottrell& Bazilevs, 2005).

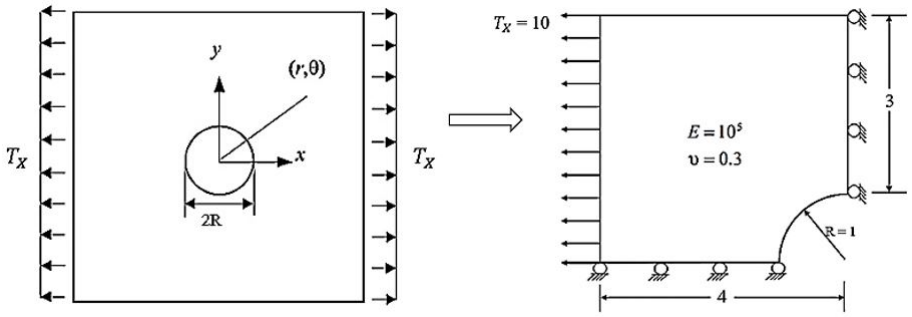

Figure 16. Elastic plate with a circular hole: problem definition. (Adapted from Hassani, Ganjali,& Tavakkoli (2011)).

The plate can be simplified in the above-mentioned configuration, and the analytical solution is presented by Chen et al. (2022):

$$\sigma_{xx} = T_x \left[1 - \frac{3R^2(x^2-y^2)}{2(x^2+y^2)^2} - \frac{R^2(x^2+y^2)^3(x^4+y^4-6x^2y^2)(1-\frac{3R^2}{2x^2+y^2})}{(x^2+y^2)^3} \right] \tag{11}$$

$$\sigma_{yy} = T_x \left[-\frac{R^2(x^2-y^2)}{2(x^2+y^2)^2} + \frac{R^2(x^2+y^2)^3(x^4+y^4-6x^2y^2)(1-\frac{3R^2}{2x^2+y^2})}{(x^2+y^2)^3} \right] \tag{12}$$

$$\tau_{xy} = -T_x \left[\frac{R^2xy}{(x^2+y^2)^2} + 4R^2xy\frac{(x^2-y^2)}{(x^2+y^2)^3} \left(1 - \frac{3R^2}{2x^2+y^2} \right) \right] \tag{13}$$

The two meshes used in this analysis consist of two quadratic isogeometric elements (a) followed by 500 cubic isogeometric elements (b) (k-refinement), in Figure 17.The Figure 18 illustrates the results obtained with the presented mesh configurations and their corresponding analytical responses.

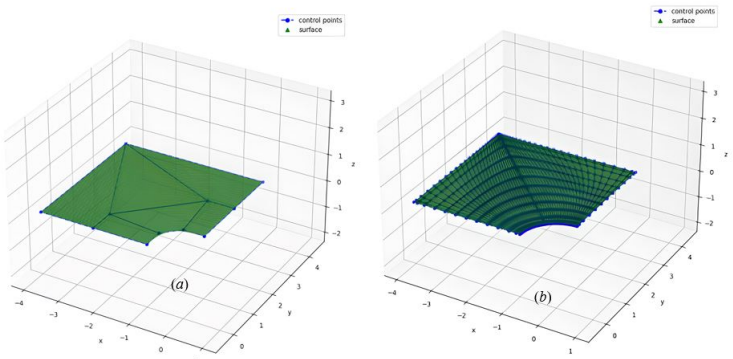

Figure 17. (a) initial mesh. (b) k-refinement mesh.

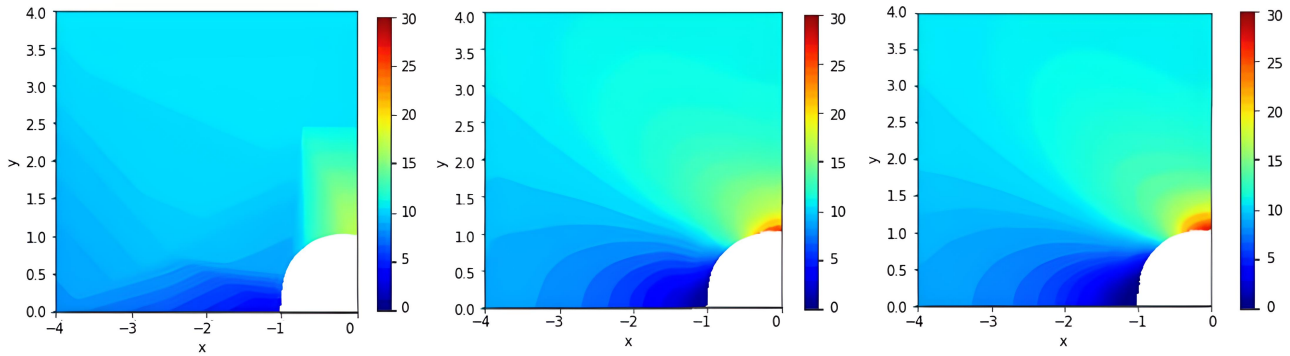

Figure 18. Contour plots of σ_{xx}: (a) initial mesh. (b) k-refinement mesh. (c) analytical solution.

As refinement of the mesh progresses, it becomes apparent that the maximum stress ($\sigma_{xx} = 30$) within the plate, situated at $r = R$ and $\theta = \frac{\pi}{2}$, converges toward the analytical solution.

6. CONCLUSION

In summary, IGA has demonstrated its effectiveness in addressing plane stress problems by employing h-refinement, p-refinement, hp-refinement, and k-refinement techniques to achieve highly accurate results. This study emphasizes that, for a classical problem in structural mechanics, precise displacement fields can be obtained by appropriately placing control points on the geometry, without the need for an overly refined mesh. Among these refinement techniques, krefinement stands out for its superior performance in reducing degrees of freedom. In the case of stress fields, especially in an infinite plate with a hole, detailed refinement with a reduced number of degrees of freedom closely approximates analytical stress distributions. Furthermore, stress distributions can be determined without the necessity of extensive mesh refinement.

Instead, this can be achieved through the application of stress recovery techniques in combination with a weighted average of stress values obtained at each control point. In this study, a simple arithmetic average of the x-component of stress was utilized. These findings affirm the efficacy of IGA in simulating and analyzing structural systems, thereby encouraging further exploration of its applications in the field of engineering.

7. ACKNOWLEDGEMENTS

The authors acknowledge the support of the Coordenação de Aperfeiçoamento de Pessoal de Nível Superior (CAPES) during the development of this research.

8. REFERENCES

References

Chen, Y.T; Li, C; Yao, L.Q; Cao, Y. A Hybrid RBF Collocation Method and Its Application in the Elastostatic Symmetric Problems. Symmetry 2022, 14, 1476. https://doi.org/10.3390/sym14071476

Cottrell, J. A.; Bazilevs, Y.; Hughes, T. J. R. Isogeometric Analysis: Toward Integration of CAD and FEA. 1st Edition. ed. USA: John Wiley & Sons, 2009.

Cottrell, J. A.; Hughes, T. J. R.; Reali, A., 2007. Studies of refinement and continuity in isogeometric structural analysis. Computer Methods in Applied Mechanics and Engineering, vol. 196.

Cottrell, J. A. et al. Isogeometric analysis of structural vibrations. Computer Methods in Applied Mechanics and Engineering, vol. 195, n. 41-43, p. 5257–5296, 2006.

Hassani, B. Ganjali, A. & Tavakkoli, M. (2011). An isogeometrical approach to error estimation and stress recovery. European Journal of Mechanics A/Solids, 21, 101-109.

Hughes, T. J. R., 2000. The Finite Element Method - Linear Static and Dynamic Finite Element Analysis. Dover Publications.

Hughes, T. J. R., & Cottrell, J. A., & Bazilevs, Y., 2005. Isogeometric analysis: CAD, finite elements, NURBS, exact geometry and mesh refinement. Computer Methods in Applied Mechanics and Engineering, vol. 194, n.39-41.

Klinkel, S. Shell formulation for Isogeometric Analysis. RWTH Aachen University, 2018.

Piegl, L., & Tiller, W., 1997. The NURBS book. Springer.

9. RESPONSIBILITY NOTICE

The authors are the only responsible for the printed material included in this paper.